NTU Journal of Renewable Energy

Available online at: https://journals.ntu.edu.iq/index.php/NTU-JRE
ISSN: 2788-9912 (print); 2788-9920 (online) Vol. 1, No. 1
DOI: https://doi.org/10.56286/ntujre.v1i1.6

RESEARCH ARTICLE
Open Access

Neural Network Based Assessment the Performance of the Triangular Integrated Collector

Raid Waadullah Daoud[1], Zaid Husain Ali[2], Zaki Majeed Abdull[3], Ahmed Hasan Ahmed[4]
raid_hwj@ntu.edu.iq[1],zaidali_hwj@ntu.edu.iq[2],drzaki_hwj@ntu.edu.iq[3],ahmedhasan_hwj@ntu.edu.iq[4]

1.Northern Technical University, Technical Institute/Hawija, Kirkuk, Iraq
Corresponding author: Raid Waadullah Daoud: ,**raid_hwj@ntu.edu.iq**
Co-authors: ZHA:zaidali_hwj@ntu.edu.iq, ZMA:drzaki_hwj@ntu.edu.iq, AHA:ahmedhasan_hwj@ntu.edu.iq.
Received: 08 August 2021, **Received in Revised form**:30 August 2021 **Accepted**: 01 September 2021,
Published online: 15 September 2021

Abstract. A numerical study was achieved on a new design of storage solar collector by using neural network (NN). The storage collector is a triangular face and a right triangular pyramid for the volumetric shape. It is obtained by cutting a cube from one upper corner at 45o, down to the opposite hypotenuse of the base of the cube. The numerical study was carried out using the computational fluid dynamics code (ANSYS-Fluent) software with natural convection phenomenon in the pyramid enclosure. The results show that, the temperature and velocity distributions throughout the operating period were obtained. The influence of introducing an internal partition inside the triangular storage collector was investigated. Also the optimum geometry and location for this partition were obtained. The enhancement was best at y= 0.25 m whereas the height of triangular collector was 0.5 m. The hourly system performance was evaluated for all test conditions. The performance of the NN to train a model for this work was 0.000207, while the error of the calculation was 1*10^-2 as average.

Keywords: Triangular, storage, solar, collector, assessment, performance.

Introduction

The cost of producing star collectors is 200 $ per sq. meter [1][2][3]. This high initial value is that the 1st downside preventing reflector to become standard for the human. It's the intent of this study to develop an occasional value, reliable, and economical star heater system for domestic use [4]. All the classical star heatersystems contain 2 main components; the collector and also the vessel. Another one prompt a replacement storage reflector for domestic predicament provide and also the collector was fictitious simply from the unremarkably out there business materials victimization easy tools and procedures. The advantage of the prompt collector style isthat it is used for water storage to switch the standard cubic or cylindrical cistern unremarkably employed in Iraqi homes. Ahmed [5] analyzed analytically and by experimentation the look of a compact reflector. Within the prompt style the collector and also the cistern are compact into one give up water flow caused by thermsyphonic action. The performance of a replacement model of the storage reflector was investigated numerically by Farhan [6]. The ANSYS software package was utilized for this assessment. Also, Ahmed [7] studied numerically and by experimentation the performance of a cylindrical compact collector in urban center town.

The invention includes AN engineering style fictitious by cutting a cube form tank at totally different orientations. During this style, the best angle of inclination is 10° to 15° over the latitude angle to gather the alternative energy within the winter season. The latitude angle for city is 31°, capital of Iraq is 33° and metropolis is 36°. Consequently, for ease and unity, a 45° common angle of inclination would be suitable [8]. The amount of the collector is controlled victimization totally different dimensions for the bottom and height at the same time. To extend the absorption of alternative energy, the sun struck surface has been painted black. The sun struck

surface is painted black to extend alternative energy absorption. A glass sheet or the other clear materials is wont to cowl the canted aspect that's facing the sun and every one the opposite sides is insulated victimization thermal insulation.

The present work was carried out to study numerically, in three dimensions, the effect of the some operational parameters on the performance of the triangular storage collector shown in Figure 1. The atlas of new designs with 4and 5links will be generated. The feasibility of new designs will be illustrated with an example, and verified by kinematic simulation.

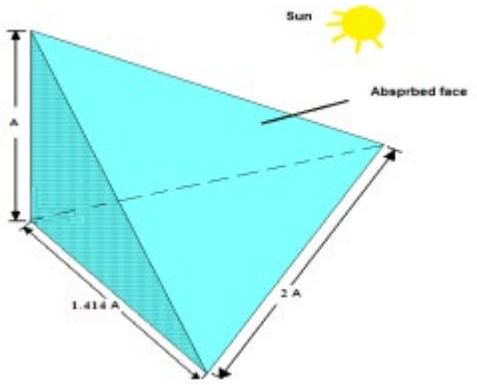


Figure 1. Schematic diagram of the triangular storage collector.

Numerical Model

The Boussinesq approximation, whereby the fluid is assumed to be Newtonian and in compressible, means the fluid density is taken as constant apart from the impact of the density variation in manufacturing buoyant forces. The density is assumed to vary solely with temperature slightly from a reference value. With these assumptions the buoyant effects, characteristic of free convection, area unit enclosed as body forces within the momentum equations. The fluid motion is assumed to be liminal owing to terribly low speed among the storage, 3 dimensional, no internal heat generation and for convenience the consequences of radiation and viscous energy dissipation area unit neglected. With these assumptions, the basic convection equations are [9]:

1- Continuity Equation:

$$\frac{\partial u}{\partial t}+\frac{\partial u}{\partial x}+\frac{\partial v}{\partial y}+\frac{\partial w}{\partial z}=0 \qquad (1$$

2- Momentum equations:

$$\frac{\partial u}{\partial t}+u\frac{\partial u}{\partial x}+v\frac{\partial u}{\partial y}+w\frac{\partial u}{\partial z}=-\frac{1}{P}\frac{\partial p}{\partial x}+v\left[\frac{\partial^2 u}{\partial x^2}+\frac{\partial^2 u}{\partial y^2}+\frac{\partial^2 u}{\partial z^2}\right]$$

$$\frac{\partial v}{\partial t}+u\frac{\partial v}{\partial x}+v\frac{\partial v}{\partial y}+w\frac{\partial v}{\partial z}=-\frac{1\partial p}{\rho\partial y}+g\beta(T-T_o)+v\left[\frac{\partial^2 v}{\partial x^2}+\frac{\partial^2 v}{\partial y^2}+\frac{\partial^2 v}{\partial z^2}\right] \qquad (2)$$

$$\frac{\partial w}{\partial t}+u\frac{\partial w}{\partial x}+v\frac{\partial w}{\partial y}+w\frac{\partial w}{\partial z}=-\frac{1}{P}\frac{\partial p}{\partial z}+v\left[\frac{\partial^2 w}{\partial x^2}+\frac{\partial^2 w}{\partial y^2}+\frac{\partial^2 w}{\partial z^2}\right]$$

3- Energy equation:

$$\frac{\partial T}{\partial t}+u\frac{\partial T}{\partial x}+v\frac{\partial T}{\partial y}+w\frac{\partial T}{\partial z}=\frac{K}{\rho * C_p}\left[\frac{\partial^2 T}{\partial x^2}+\frac{\partial^2 T}{\partial y^2}+\frac{\partial^2 T}{\partial z^2}\right]$$

(3)

In the finite volume method, the above equations are treated in a balanced form for finite-sized control volumes (CV). Equations 1, 2, and 3 can be rewritten as:

$$\frac{\partial(\rho\varphi)}{\partial t}+\frac{\partial(\rho u\varphi)}{\partial x}+\frac{\partial(\rho v\varphi)}{\partial y}+\frac{\partial(\rho w\varphi)}{\partial z}=\frac{\partial}{\partial x}(\Gamma\frac{\partial\varphi}{\partial x})+\frac{\partial}{\partial y}(\Gamma\frac{\partial\varphi}{\partial y})+\frac{\partial}{\partial z}(\Gamma\frac{\partial\varphi}{\partial z})+S \qquad (4)$$

The fully implicit discretization equation for a typical control volume is shown as follows:

$$a_P\varphi_P=a_W\varphi_W+a_E\varphi_E+a_S\varphi_S+a_N\varphi_N+a_B\varphi_B+a_T\varphi_T+a_\beta\varphi_\beta+S_U \qquad (5)$$

Re-write the above equations in the following terms:

$$\frac{\partial(\rho\varphi)}{\partial t}+\mathrm{div}(P\varphi u)=\mathrm{div}(\Gamma\mathrm{grad}(\varphi))+S \qquad (6)$$

The storage solar collector complex geometry requires computational fluid dynamics approach. Standard correlations of heat transfer cannot adequately describe the natural convection within the solar storage collector. A commercial package of CFD (Fluent) was used to model the collector in this study with the utilization of Gambit software for mesh generation. The triangular collector grid was built as in Figure (2).



Figure 2. Mesh model of the triangular collector.

During this model, tetrahedral part kind was chosen employing a lily-white problem solver with the implicit formulation. The second order theme was wont to solve the momentum and energy equations. Buoyancy-driven flow is thought as natural convection flow and also the Boussinesq approximation is employed for density. The discretization of the body force weighted theme is usually recommended to resolve high John William Strut variety flows. Consequently, the body force weighted theme was enforced to discretize the pressure term. Pressure-implicit with the cacophonic of operators (PISO) algorithmic program that is usually recommended for transient flow calculation was wont to accomplish the pressure-velocity coupling. So as to regulate the variable fluctuations and avoid divergence of solutions throughout ordered iterations, under-relaxation factors were applied. Once resolution the equations, the everyday under-relaxation parameter values used were roughly zero.3 and 0.7 for pressure and momentum, severally, and 0.8 for each energy and density.

Methodology

The NN were used in this work as a prediction model to discover the main temperature which must be reached for the given parameters (time and size). The Elman back propagation network is used for his ability to find the nearest solution with smallest error rate. The network shown in Figure (3) represent the three layers with the corresponding weights. There are only one input and one output for the network to study the effect of the time and size of the collector on the overall behavior of the system individually.

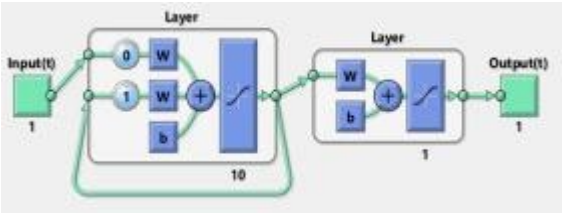


Figure 3. Elman network with the I/P, hidden and O/P layer.

Results and Discussion

The hourly incident solar radiation on a titled surface for 365 days was obtained by a computer program developed in this work based on the ASHRAE clear sky model. The volume of the triangular collector is 41.667 liters and the sunlit area is 0.353 m2 at a height (A) of 0.5 m. All results were evaluated fora typical winter days (13th, 14th, 15th and 16th of November). The hourly incident solar radiation on a titled surface for 365 days was obtained by a computer program developed in this work based on the ASHRAE clear sky model. The volume of the triangular collector is 41.667 liters and the sunlit area is 0.353 m2 at a height (A)

1. Effect of Collector Volume

Figure (4) shows the relation between the mean storage temperature and the heights of the collector. A varying height and base dimensions renders varying storage volumes. It is observed that the mean storage temperature decreased with increasing volume. It is observed that the mean storage temperature reaches its maximum value at A=0.5 m, where the collector volume is 41.67 liters. The minimum is obtained for a collector with A=1 m, where the collector volume is 333.33 liters. Also, the results predictions show that the stratified behavior of the collector becomes weaker with increasing volume, as shown in Figure (5).

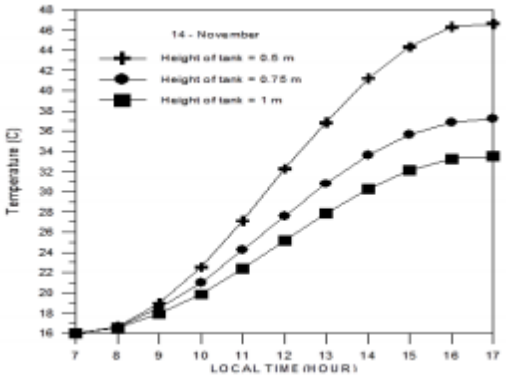
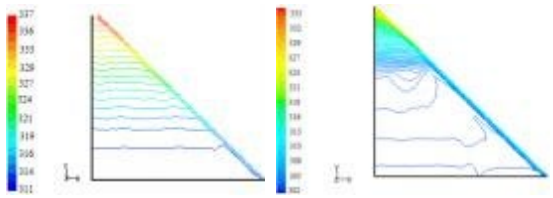


Figure 4. Variation of mean storage temperature for various volumes

The NN output satisfy the numerical conditions and its response exactly same the conventional values, as shown in Figure (6).

The three curves shown in Figure (5) represent the NN response with respect to collector size and time as mentioned in the figure graph and legend. The curves has a big similarity which means a very error rate within the NN computation. The system performance and validation accuracy were fixed during the training process is shown in Figure (7) below.



(a) Isothermal temperature lines at symmetry plane A-A forA=0.5 m.

(b) Isothermal temperature lines at symmetry plane A-A forA=1 m.

Figure 5. Storage water stratification inside the Triangular collector

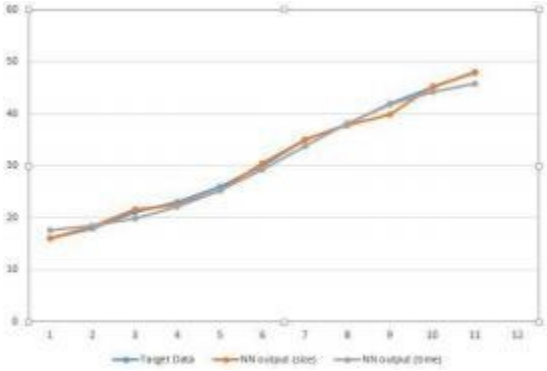


Figure 6. The NN response with respect to size and temp.

The validation represent the optimized solution that can be fixed to obtain on the best system efficiency. The agreement between the numerical predictions and the experimental data is good up to 2 p.m. as shown from Figure (8). Also, it is noted that a larger volume means the water capacity increases, and hence the storage water temperatures at the end of day decreases and vice versa. This is shown in Figure 6. It is interesting to note that as the volume increases the collection efficiency increases as shown in Figure (9) because the thermal losses to the outside air decrease.

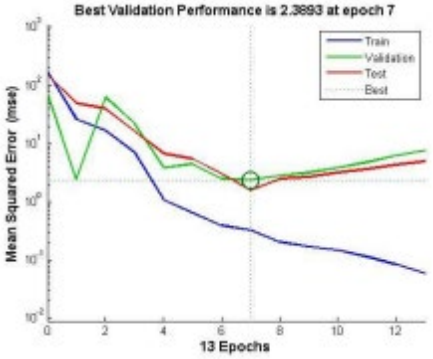


Figure7. The NN train, test and validation process and point of solution.

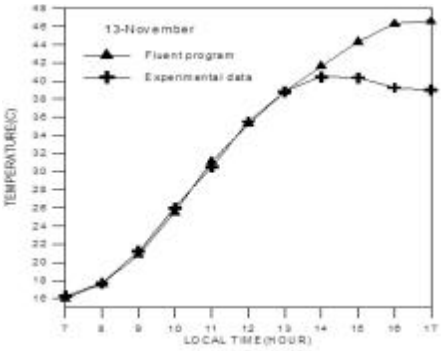


Figure 8. Numerical and experimental variation of the mean storage temperature.

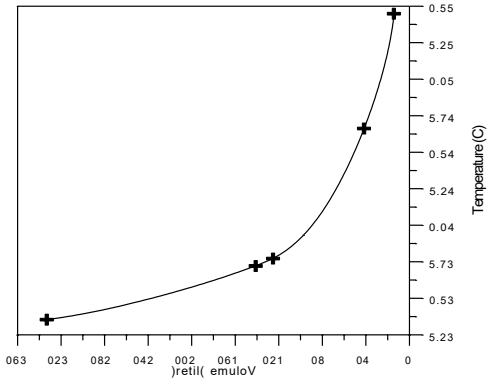


Figure 9. The relation between the mean storage temperature and the collector volume

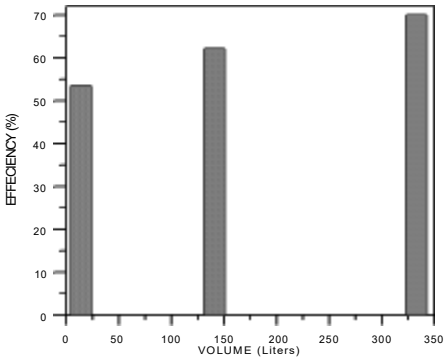


Figure 10. The relation between overall efficiency and the collector volume.

2. Effect of the Internal Partition

It was suggested to investigate the influence of using an internal partition inside the collector and study its influence on the temperature distribution and collector performance. This was done by using an internal partition with certain heights positioned in different locations as shown in Figure (11) Giving four different cases. All tests were carried out for a typical cold day.

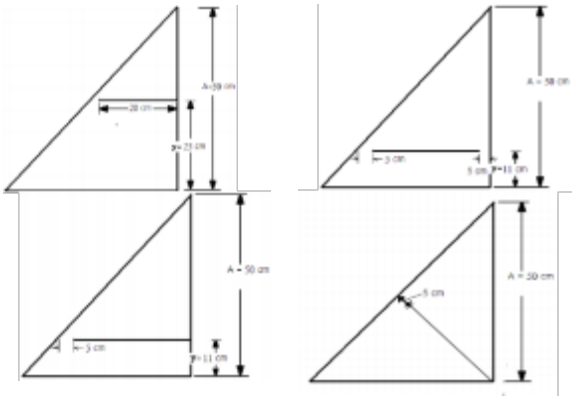


Figure 11. Shows the various locations of partitions.

The mean storage temperature will be used as a criterion for assessment. It is observed that, when the partition is in a position which separates the collector into two equal volumes as in cases 2 and 3, there is no clear effect of the partition on the storage water temperature as shown in Figure (12). The influence of the internal barrier is pronounced in cases 1 and 4, whereby an increase in the mean storage temperature is obtained. The separation between the hot and cold water causes this increase. It is noticed from Figure (12) That the mean storage temperature for case (1) reaches 49 °C, which is higher than for other cases.

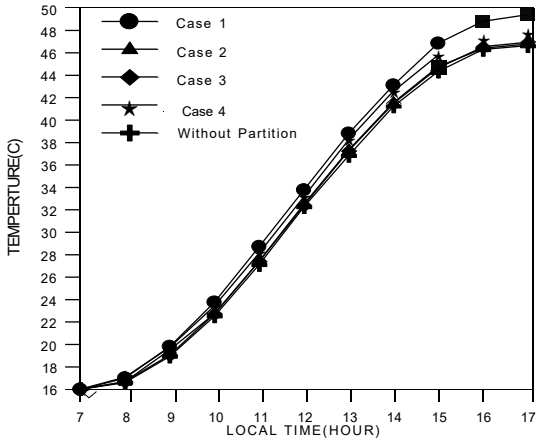


Figure 12. shows the barrier effect on the mean storage temperature.

Figure (13) shows the effect of the barrier on the maximum temperature atthe top of the collector. As shown, the maximum temperature was at 2 p.m. and reduced at the end of the operation period.

Figure (14) shows the temperature distribution of water in a triangular tank at 3 p.m. for a typical cold weather. The partition of the case (1) hinders direct circulation between warm and cold fluid, which is a useful result in positioning the cold- water inlet and the hot water outlet. Also, it shows that mainly at no load condition, the cold water is confined below the partition while the warm water is above the barrier.

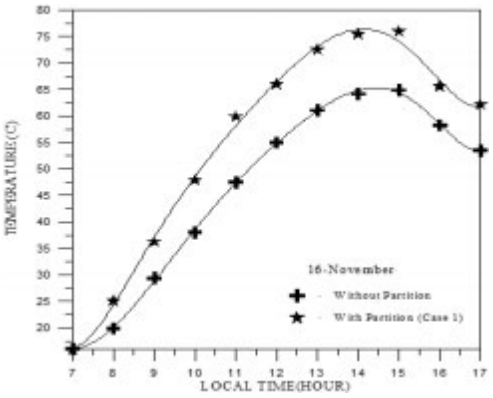


Figure 13. Effect the effect of partition on the max temperature in case 1.

It is noticed that the temperature difference between the top and bottom of the collector increased significantly as compared with the no partition case. Also, the stratification in the collector was not disturbed by the existence of the adiabatic partition [10].

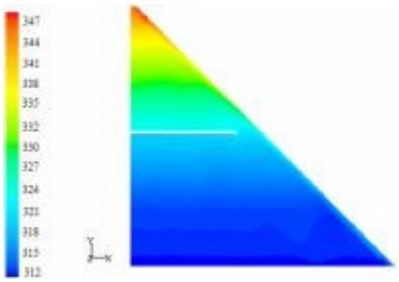


Figure 14. shows the effect of partition on temperature distribution (K) in a symmetry plane for case 1.

Figure (15) shows the flow of water inside the system at 2 p.m. for a typical winter day. The flow included three relatively distinct regions (A, B and C) as denoted on this figure. The flow in region A is laminar and moves along the inclined surface and then turns left to perform an anticlockwise circulation inside the collector at the base. The second and third regions, B and C are characterized by complex random motion. The presence of the partition hinders the particle motion from region B to C or vice versa.

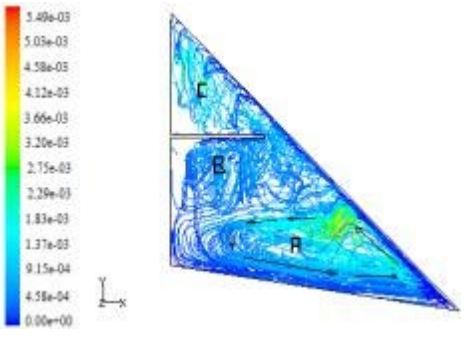


Figure 15. shows the effect of partition on particle motion.

3. Effect of Nocturnal Cooling on Triangular Collector Performance

The intimate contact between the storage fluid and the absorber plate in the storage collector facilitates efficient solar conversion but can also lead to substantial heat losses during periods of low and/or zero solar radiation particularly at night. Convective heat exchange with the ambient air and radiated heat transfer to the cold night sky are the significant mechanisms of heat losses. This effect can be reduced, to some extent, by covering the transparent face of the system by a removable insulating cover such as cork of 50 mm thickness. It can be removed early in the next day so that the water remains warm until the next morning. The dynamic response of the system during such cooling hours was analyzed by doing the transient study of the system and carrying out the following tests:

1- Transient study without an insulating cover.

2- Transient study with an insulating cover.

In test 2, it was assumed that the collector was covered by insulation at 5 p.m. and it was removed next day at about 7 a.m. During test 1, it was assumed that the front face was without any cover. Figure (16) shows the performance of the system with and without insulating cover for different volumes of the triangular collector. Water temperature rises up to 46.6, 37.25 and 33.5 °C respectively for 41, 141 and 333 liters, at about 5 p.m. in the afternoon. This temperature falls to 34.8, 32.9 and 30.6 °C in the next morning when these systems are left uncovered during nighttime.

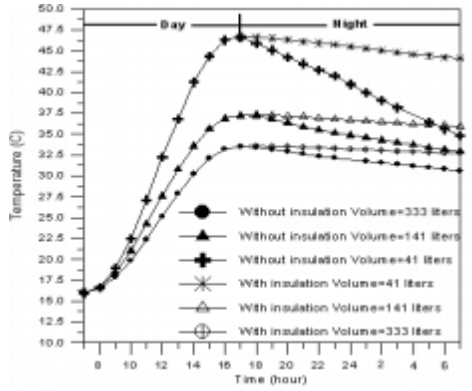


Figure 16. Shows the effect of insulating transparent cover during the off period on mean storage temperature.

But when this collector is covered with insulation of 5 mm thickness, the water temperature falls to 44.1, 35.9 and 32.67 °C respectively as in table I. It means that the fall in water temperatures which were 11.83, 4.32 and 2.9 °C have been reduced to 2.55, 1.3 and 0.87 °C, respectively. The reduction in heat losses is a function of the volume of the collector. Since the decrease of water temperature is small in the case have 141 and 333 liters volumes of the collector, then the use of insulation cover is not very promising.

Most Iraqi houses contain a storage tank situated over the roof of the house for storing the water. The current system can also be used for storing water. During summer, the water temperature rises up to levels that prevent use of this water for drinking and other house purposes. An experiment has been conducted to determine average temperature rise for the collector for the 14th of June. The tank was filled at 6 a.m. and the transparent face was covered throughout the day. The mean storage temperature rose from 26 °Cto 31 °C. Thus, using this system could considerably reduce the energy required to reduce water temperature in house cooler.

4. Effect of nocturnal cooling on mean storage temperature in the next morning

Table 1. cover effect on the collector

Collector volume (liters)	Mean Storage Temperature (°c)	
value	Without cover (°C)	With cover (°C)
41	34.8	44.1
141	32.9	35.9
333	30.6	32.67

Conclusions

From the obtained results, we can conclude the following notes can be observed:

1. The presence of a horizontal barrier inside the triangular storage collector increases stratification of water and renders a higher mean storage temperature. The enhancement was best at y = 0.5 m. The mean storage temperature for case (1) reaches 49 °C, which is higher than for other cases.
2. Stratification behavior diminishes with increasing volume because the turbulent effect begins to appear.
3. Covering the sunlit area of the system with insulation during nighttime improves the performance. Water temperature rises up to 46.6, 37.25 and 33.5 °C respectively for 41, 141 and 333 liters, at about 5 p.m. in the afternoon. This temperature falls to 34.8, 32.9 and 30.6 °C in the next morning when these systems are left uncovered during nighttime.

4. Test and validation for the system behavior gives a big reliability during the NN and satisfying the conventional conditions.

REFERENCES

[1] A. A. Adeyanju, "Economic analaysis of combined packed bed energy storage and solar collector system," International Journal of Renewable energy Research, vol. 3, no. 4, 2013.

[2] O. K. Ahmed and A. H. Ahmed, Principles of Renewable energies, First edit. Baghdad: Foundation of technical education, 2011.

[3] O. K. Ahmed and Z. A. Mohammed, "Influence of porous media on the performance of hybrid PV/Thermal collector," Renew Energy, vol. 112, pp. 378–387, 2017.

[4] Omer K. A., Raid W. D., Sameer A., "Design and simulation of a predictive system to determine the basic factors of solar cells using neural networks," Sustainable Resources Management Journal, vol. 3, pp. 79–87, 2018.

[5] O. K. Ahmed, "Assessment of the performance for a new design of storage solar collector," International Journal of Renewable energy Research, vol. 8, no. 1, pp. 250–257, 2018.

[6] K. A. Joudi, I. A. Hussein, and A. A. Farhan, "Computational model for a prism shaped storage solar collector with a right triangular cross section," Energy Convers Management, vol. 45, no. 3, pp. 391–409, 2004.

[7] O. K. Ahmed, "Experimental and numerical investigation of cylindrical storage collector (case study)," Case Stud Therm Engineering, vol. 10, pp. 362–369, 2017.

[8] O. K. Ahmed and S. M. Bawa, "Reflective mirrors effect on the performance of the hybrid PV/thermal water collector," Energy Sustain Development, vol. 43, pp. 235–246, 2018.

[9] O. K. AHMED and S. M. BAWA, "The combined effect of nano-fluid and reflective mirrors on the performance of PV/Thermal solar collector," Thermal Science, pp. 1–16, 2018.

[10] J. Varghese and K. Manjunath, "Experimental investigation and comparison between an integrated compound parabolic domestic solar water heater with and without an air gap introduced at the arms of the CPC," International Journal of Advanced Research Innovation, vol. 5, no. 1, pp. 90–93, 2017.